Burst detection and localization in water pipelines based on an extended differential evolution algorithm

A. Badillo-Olvera, A. Pérez-González, O. Begovich and J. Ruíz-León

ABSTRACT

This paper presents a new burst detection and location technique for pressurized pipelines based on an extension of the Differential Evolution (DE) algorithm. The proposed approach addresses the burst location problem as an optimization task, by considering the dynamic model that describes the behavior of a fluid through a pipeline and the presence of fluid losses produced by a burst. The optimization problem relies on finding suitable estimations related to the burst parameters, i.e. magnitude, pressure and position of a burst, while a defined cost function is minimized. In order to deal with this problem, three strategies are proposed to extend and adapt the DE algorithm: (i) an informed definition of the physical restrictions of the problem according to the pipeline characteristics; (ii) a training stage of the algorithm that allows to find the appropriate synthesis parameters; (iii) a multi-start structure, in order to track dynamical variations of the problem. Experiments on a pipeline prototype illustrate the results obtained by the proposed algorithm on the estimation of the burst parameters, comparing its performance with an algorithm based on the Extended Kalman Filter, which is widely used in the literature.

Key words | evolutionary methods, fault-diagnosis, fluid losses, parameter estimation, water pipeline monitoring

A. Badillo-Olvera (corresponding author)
A. Pérez-González
O. Begovich
J. Ruíz-León
Cinvestav-IPN,
Unidad Guadalajara,
Av. del Bosque 1145 Col. El Bajío, 45019 Zapopan, Jalisco,
México
E-mail: *ambadillo@gdl.cinvestav.mx*

INTRODUCTION

Water loss management is one of the most important issues facing water suppliers around the world. In many water pipelines, a significant percentage of the total water volume supplied is lost due to bursts and leaks, resulting in discontinuous, expensive and inefficient services. Furthermore, the presence of a burst can lead to the rapid deterioration of the pipeline, which might allow contaminant ingress and affect the urban infrastructure (Xie *et al.* 2017). Therefore, in the current literature, different works are focused on developing leak and burst diagnosis algorithms. These algorithms have a common objective to detect and locate leaks or bursts automatically in transmission pipelines, with good precision and minimum invasion of the pipeline (e.g. Verde 2001; Wang *et al.* 2002; Kowalczuk & Gunawickrama 2004; Torres *et al.* 2014; Navarro *et al.* 2017; Brunone *et al.* 2018; Lizarraga-Raygoza *et al.* 2018). In general, there are two widely used approaches to address the burst diagnosis problem, the Transient Test Based (TTB) and the Fault Model Approach (FMA). The idea of the TTB is to exploit the information of the transient produced by burst (Wang *et al.* 2002; Brunone *et al.* 2015, 2018), where the governing equations are expressed in terms of a Fourier series, and it is distinguished the deviation of the damping characteristics to the burst occurrence from the damping characteristics of the normal operation conditions. On the other hand, the FMA is based on the use of an analytical representation of the dynamic behavior of the flow rate and the pressure head in a pipeline, where the effect of a possible burst that affects the pipeline dynamics is considered within the model. This makes possible a direct estimation of the burst parameters (Santos-Ruiz *et al.* 2018). The extended Differential Evolution (DE)

doi: 10.2166/hydro.2019.123

algorithm proposed to address the Burst Diagnosis and Location (BDL) problem in the present paper is focused in the FMA.

In general, burst detection and localization algorithms based on the FMA are developed under different design considerations and mathematical assumptions. However, in real applications, these considerations are not always fulfilled, causing a reduction in the algorithms reliability and precision. Then, it is convenient to use algorithms developed under different estimation techniques that can work in parallel (analytical redundancy) in order to offer a more informed and reliable diagnosis (Carvajal-Rubio & Begovich 2016; Santos-Ruiz *et al.* 2018). This fact motivates the development of new techniques to address the burst detection and location problem in transmission pipelines. In view of the above, the main contribution of this paper is *the development of a new BDL algorithm based on an extended DE algorithm and under FMA, which presents characteristics such as reliability, easy implementation and simple configuration*. As far as we know, the use of heuristic techniques to address the BDL problem has not been explored before.

The DE algorithm has been widely applied in the water management and optimal design of water distribution systems (Suribabu 2010; Zheng *et al.* 2011). In this paper, the DE algorithm is proposed to address the burst detection and localization problem as an optimization task that relies on finding suitable estimations related to the magnitude, pressure and position of a burst, while a proposed cost function is minimized. This algorithm addresses the optimization problem through a sequence of evolutive operations (mutation, recombination and selection) in order to find the candidate solution with the best cost function evaluation.

In order to achieve feasible solutions with a low number of iterations, the present paper also proposes a three-step procedure to improve the adaptation of the classical DE algorithm in the BDL problem. These steps are: first, the boundaries of the search space are carefully proposed as a set of restrictions of the optimization problem according to the physical characteristics and mechanical properties of the pipeline. The boundaries of the search space play a fundamental role in the performance of the DE algorithm. Thus, by providing informed bounds, as a priori knowledge, the DE algorithm can reach a good feasible solution in a short time. Second, to select the appropriate synthesis parameters for the DE algorithm, a training step is performed using the method presented by Pérez-González *et al.* (2019). This method consists in evaluating the performance of the algorithm in a particular case, under an iterative execution that uses different synthesis parameters. The information acquired from the iterative execution allows to find the values of the parameter settings where few iterations are needed to approximate a solution to the problem. On the other hand, the BDL problem as an optimization task requires a special consideration due to its dynamic characteristics. Therefore, the proposed algorithm includes, as its third strategy, a multi-start structure that allows to track the pressure dynamical variations in the burst point. The proposed burst diagnosis method based on the extended DE algorithm is implemented and evaluated in a pipeline prototype installed at Cinvestav, Guadalajara, México. As it will be shown, the obtained results illustrate the effectiveness of the proposed algorithm compared with the Extended Kalman Filter (EKF), which is widely used for the burst diagnosis problem.

The paper is organized as follows: Preliminaries section presents the pipeline dynamic model, introduces the BDL problem, and describes the classical DE algorithm. In the Burst parameter identification strategy section, the improved DE algorithm to tackle the BDL problem solution is presented. The Experiments and results section presents and discusses the results obtained. Finally, the respective conclusions are stated.

PRELIMINARIES

This section introduces the burst detection and localization problem, starting with a brief description of the pipeline fluid dynamic equations, and afterwards the model considered in this work to address the BDL problem is introduced. Also, a brief description of the classical DE algorithm is presented.

Pipeline model

The equations describing the transient pressure and flow rate in closed conduits are a set of partial differential equations known as Water Hammer Equations (WHE), which are derived applying the conservation laws on a control volume (Roberson *et al.* 1998). In general, the transient

flow is considered unidirectional since the terms of the convective acceleration are smaller than the axial terms. Therefore, by neglecting these terms and the spatial density variation, besides considering a fluid slightly compressible, pipes slightly deformable, and a leveled pipeline, the WHE can be expressed as (Chaudhry 2014):

$$\frac{a^2}{gA}\frac{\partial Q(z,t)}{\partial z}+\frac{\partial H(z,t)}{\partial t}=0 \tag{1}$$

$$\frac{\partial Q(z,t)}{\partial t}+gA\frac{\partial H(z,t)}{\partial z}+J_w(z,t)=0 \tag{2}$$

where a is the pressure wave speed in the fluid $[m/s]$, A is the cross-sectional area of the pipeline $[m^2]$, Q is the flow rate $[m^3/s]$, z is the spatial coordinate along the pipeline $[m]$, g is the gravitational acceleration $[m/s^2]$, H represents the pressure head $[m]$, t is the temporal coordinate $[s]$, J_w represents the friction factor head losses [*dimensionless*], and D is the diameter of the pipe $[m]$.

The pressure wave speed can be approximated by different formulations; however, the precision of the estimations highly depends on the mechanical properties of the material, which change with the pipeline deterioration. Furthermore, in plastic materials, the pressure wave speed estimations present variations in comparison with the values suggested in classical textbooks (Evangelista *et al.* 2015). Therefore, different authors as Meniconi *et al.* (2015) and Soares *et al.* (2008) propose experimental procedures in order to obtain more suitable pressure wave speed estimations.

In order to compute friction effects for transient flow conditions, different methods have been developed. In general, the friction losses are divided into quasi-steady (J_s) and unsteady (J_u) parts, as $J_w = J_s + J_u$. The quasi-steady term is usually estimated by the Darcy–Weisbach equation:

$$J_s = f\frac{Q|Q|}{2DA} \tag{3}$$

where the friction factor f can be estimated by the Swamee and Jain equation:

$$f=\frac{0.25}{\left[\log_{10}\left(\frac{\varepsilon/D}{3.7}+\frac{5.74}{Re^{0.9}}\right)\right]^2} \tag{4}$$

where Re is the Reynolds number obtained from $R_e = QD/(\nu A)$, ν is the kinematic viscosity $[m^2/s]$ and ε is the roughness coefficient of the pipe material $[m]$. On the other hand, different formulations (e.g. Brunone *et al.* 1995; Duan *et al.* 2017) have been proposed to compute the unsteady part J_w. In this way, Dulhoste *et al.* (2011, 2017) present a study that evaluates the influence of the friction unstable term in the implementation of leak location algorithms based on observers and developed under the FMA. Based on their results, the authors conclude that the unsteady formulation is complex and it only presents a small improvement in the burst diagnosis. In view of the above, the present paper neglects the unsteady friction term.

Burst localization model

In order to develop a model based on FMA, it is necessary to consider the burst effect into a model. When a pipe burst occurs, a sudden pressure wave is generated and propagated in both directions from the burst point. This behavior induces spatial and temporal changes in the velocity flow rate and the pressure, i.e. transients, until a new stable state, is reached. This new stable state depends on the burst size and magnitude. A widely used model in practical and real scenarios (e.g. Torres *et al.* 2014; Delgado-Aguiñaga & Begovich 2017; Verde & Torres 2017; Santos-Ruiz *et al.* 2018), that takes into account the burst effects, is deduced from the spatial discretization of the WHE through the explicit Finite Differences method and then incorporating the effect of the burst.

The effect of an orifice of constant diameter produced on the burst flow rate can be obtained by using the general orifice equation as the classical leak model (Ferrante *et al.* 2014):

$$Q_L = \lambda\sqrt{H_L} \tag{5}$$

where $\lambda \doteq C_d A_L \sqrt{2g}$ is a factor associated with the burst magnitude, A_L is the orifice area $[m^2]$, H_L is the pressure head at the burst point $[m]$ and C_d is the discharge coefficient [*dimensionless*].

Considering a pipeline discretization in two sections, as shown in Figure 1, the WHE can be approximated by the

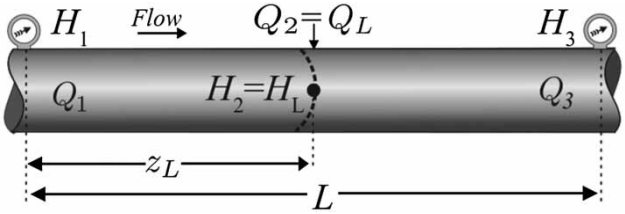

Figure 1 | Spatial discretization of a pipeline in two sections.

next nonlinear model:

$$\begin{bmatrix} \dot{Q}_1 \\ \dot{H}_2 \\ \dot{Q}_3 \end{bmatrix} = \begin{bmatrix} -\frac{gA}{z_L}(H_2 - u_1) - f\frac{(Q_1)}{2DA}Q_1|Q_1| \\ -\frac{1}{z_L}\left(\frac{a^2}{gA}\right)\left(Q_3 - Q_1 + \lambda\sqrt{H_2}\ \right) \\ -\frac{gA}{L - z_L}(u_2 - H_2) - f\frac{(Q_3)}{2DA}Q_3|Q_3| \end{bmatrix} \tag{6}$$

where z_L is the distance from the beginning of the pipeline to the burst position, $u = [H_1 \quad H_3]^T$ is the input vector that contains the pressures at the ends of the pipeline, $y = [Q_1 \quad Q_3]^T$ is the output vector that contains the flow rates and $f(Q_1)$ and $f(Q_3)$ represent the friction coefficients calculated with the input and output flows, respectively.

In this work, the proposed method only considers a single burst. Equation (6) can be written in the classical form of a nonlinear state space representation:

$$\begin{aligned} \dot{x} &= \xi(x, u) \\ y &= Cx \end{aligned} \tag{7}$$

where $x \doteq [Q_1 \quad H_2 \quad Q_3]^T$, $C = \begin{bmatrix} 1 & 0 & 0 \\ 0 & 0 & 1 \end{bmatrix}$ and $\xi(\cdot)$ is a nonlinear function.

To obtain a computationally feasible representation of model (6), a temporal discretization based on the Heun's method is performed as in Delgado-Aguiñaga *et al.* (2015), as follows:

$$\begin{aligned} \hat{Q}_1(k+1) = Q_1(k) + \frac{\Delta t}{2}\Bigg[& -\frac{gA}{z_L}(H_2(k) - u_1(k)) \\ & -\frac{f(Q_1(k))}{2DA}(Q_1(k)|Q_1(k)|) - \frac{gA}{z_L}(\tilde{H}_2(k+1) - u_1(k+1)) \\ & -\frac{f(\tilde{Q}_1(k+1))}{2DA}(\tilde{Q}_1(k+1)|\tilde{Q}_1(k+1)|)\Bigg] \end{aligned}$$

$$\begin{aligned} \hat{H}_2(k+1) = H_2(k) + \frac{\Delta t}{2}\Bigg[& -\frac{a^2}{gAz_L}\left(Q_3(k) - Q_1(k) + \lambda\sqrt{H_2(k)}\right) \\ & -\frac{a^2}{gAz_L}\left(\tilde{Q}_3(k+1) - \tilde{Q}_1(k+1) + \lambda\sqrt{\tilde{H}_2(k+1)}\right)\Bigg] \end{aligned}$$

$$\begin{aligned} \hat{Q}_3(k+1) = Q_1(k) + \frac{\Delta t}{2}\Bigg[& -\frac{gA}{L - z_L}(u_2(k) - H_2(k)) \\ & -\frac{f(Q_3(k))}{2DA}(Q_3(k)|Q_3(k)|) - \frac{gA}{L - z_L}(u_2(k+1) - H_2(k+1) \\ & -\frac{f(\tilde{Q}_3(k+1))}{2DA}(\tilde{Q}_3(k+1)|\tilde{Q}_3(k+1)|)\Bigg] \end{aligned} \tag{8}$$

where

$$\tilde{Q}_1(k+1) = Q_1(k) + \Delta t \left[-\frac{gA}{z_L}(H_2(k) - u_1(k)) - \frac{f(Q_1(k))}{2DA}(Q_1(k)|Q_1(k)|)\right]$$

$$\tilde{H}_2(k+1) = H_2(k) + \Delta t \left[\frac{a^2}{gAz_L}\left(Q_3(k) - Q_1(k) + \lambda\sqrt{H_2(k)}\right)\right],$$

$$\tilde{Q}_3(k+1) = Q_3(k) + \Delta t \left[-\frac{gA}{L - z_L}(u_2(k) - H_2(k)) - \frac{f(Q_3(k))}{2DA}(Q_3(k)|Q_3(k)|)\right]$$

and k is the index of the discrete time and Δt is the time step. Model (8) can be written in compact form as follows:

$$x(k+1) = \xi_d((x(k), u(k), u(k+1)), y(k) = Cx(k) \tag{9}$$

where $x(k) = [Q_1(k) \ H_2(k) \ Q_3(k)]$, $u(k) = [H_1(k) \ H_2(k)]^T$ and $\xi_d(\cdot)$ is a nonlinear function.

In a practical scenario, the typical instrumentation of a transmission pipeline is composed of pressure and flow rate sensors located at the ends of the pipeline. The main objective of this sensor configuration is to evaluate the supplied volumes to the distribution zones and to monitor the efficiency of the system. This pipeline instrumentation scheme is suitable for the use of model (9) in the implementation of a BDL algorithm. Also, it is necessary that the sampling rate satisfies the Courant–Friedrichs–Lewy (CFL) criterion in order to guarantee the numerical stability of model (9). The CFL condition can be expressed as: $\Delta z \geq a\,\Delta t$, where Δt is the time step.

Longitudinal adjustment

In general, pipeline systems are composed of different fittings in order to adapt the installation to the topography features. When the fluid flows through a fitting, such as a contraction or an elbow, the viscous effects and the turbulence produced by the shape of these accessories cause an energy loss, known as a *local loss*, which is added to the friction produced in the straight pipe sections. The WHE are developed considering a straight pipeline, without accessories. Thus, in order to obtain a dynamical model that includes fittings, in terms of the WHE, it is necessary to express the length of the pipeline in an *equivalent straight length* (L_{eq}). Hence, each accessory in the studied pipeline will be seen as a virtual straight pipe section that generates the same local loss associated with its corresponding accessory (Mataix 1982). Following this, L_{eq} is computed by using the Darcy–Weisbach equation:

$$L_{eq} = \frac{\Delta H D^5 \pi^2 g}{8 f Q^2} \tag{10}$$

where ΔH is the differential head pressure at the ends of the pipeline in a burst-free condition [m]. Finally, by letting $L = L_{eq}$ in Equation (8), it is possible to introduce the effects of the fittings into the pipeline model.

Using the longitudinal compensation, the burst is localized in a virtual equivalent straight length, however, in a practical situation, this does not represent a complete solution. In addition to the burst localization, it is necessary to establish a conversion from the obtained virtual position to a real-length value. In this work, we use the procedure described by Badillo-Olvera *et al.* (2017) in order to perform this conversion.

Differential Evolution algorithm

The DE is a powerful optimization algorithm, which has proved to be very robust in a wide variety of problems (Price *et al.* 2006; Coello *et al.* 2007); furthermore, it only needs two control synthesis parameters, which makes it easy to configure. In general, the DE algorithm is used to address problems in which the decision variables are real numbers and this feature is suitable to address the BDL problem. In the DE algorithm, the candidate solutions play the role of individuals, being classified according to an objective function f_c. This classification ensures the survival of the elements with the best performance, driving the evolution in a set of greedy directions.

The DE algorithm maintains the general scheme of an evolutionary method considering a population, of the form $\chi_{\{i,g\}} = [\chi_{\{i,1,g\}}, \chi_{\{i,2,g\}}, \ldots, \chi_{\{i,d,g\}}]^T$, where $i = 1, 2, \ldots,$ NP is an integer index that distinguishes each individual from the other members of the NP-size population, g is the generation index and d is the dimension of each individual, given by the number of parameters to be optimized, that is, each element of each individual corresponds to an unknown parameter of the optimization problem. The initial population $g = 0$ is generated by a uniform random process, settled in the interval $\{\chi_j^{low} \leq \chi_{i,j,0} \leq \chi_{j^{up}}\}$ for $j = 1, 2, \ldots, d$. After the initialization, the DE process becomes an iterative sequence of evolutionary operations based on mutation, recombination, and selection (Zhang & Sanderson 2009). This process will be described as follows.

- *Mutation:* In this step, mutant vectors $v_{i,g} = [v_{i,1,g}, v_{i,2,g}, \ldots, v_{i,d,g}]^T$ are calculated at each g generation, based on the current population χ_{ig}. In this work, the mutation strategy denominated by Price *et al.* (2006) as *DE current-to-best/1* is used. This technique considers the candidate solution with the best performance found at the moment, χ_{best}, as part of the mutation operation, in addition to a randomized contribution. The equation that describes this process is as follows:

$$v_{i,j,g} = \chi_{i,j,g} + F(\chi_{best,j,g} - \chi_{i,j,g}) + F(\chi_{r1,j,g} - \chi_{r2,j,g}) \tag{11}$$

  where r_1 and r_2 are positive integers from a uniform random distribution in the interval [1, NP], F is the mutation factor, which usually ranges in the interval [0,2]. In general, the ability to perform local searches (exploitation) is achieved through values of F near to 0 and, on the contrary, the global search (exploration) is given by fixing F near to 2.
- *Recombination:* In order to improve the diversity of the population, a recombination process is defined after the mutation step, performing a crossover operation in each individual $\chi_{i,g}$, by using as its partner the mutant vector $v_{i,g}$. This operation generates a trial vector

$\mu_{i,g} = [\mu_{\{i,1,g\}}, \mu_{\{i,2,g\}}, \ldots, \mu_{i,d,g}]^T$ by means of:

$$\mu_{i.j.g} = \begin{cases} v_{i,j,g}, & \text{if} \quad \text{rand}(0, 1) < C_r \\ \chi_{i,j,g}, & \text{otherwise} \end{cases} \tag{12}$$

where C_r is the *crossover rate*, which is a constant fixed in the interval [0, 1], and it controls the admittance of the entries from the mutant vector in the formation of the trial vector.

- *Selection:* In order to determine the best candidate solutions that will pass to the next generation $g + 1$, each trial vector $\mu_{i,j,g}$ is compared against its corresponding parent, as follows:

$$\chi_{i,g+1} = \begin{cases} \mu_{i.g}, & \text{if } f_c(\mu_{i,g}) < f_c(\chi_{i,g}) \\ \chi_{i,g}, & \text{otherwise} \end{cases} \tag{13}$$

The processes of mutation, recombination and selection are iteratively executed until the optimum parameters are obtained or a pre-specified stop criterion is satisfied.

BURST PARAMETER IDENTIFICATION STRATEGY

The general formulation of identification techniques is based on the comparison between the response of a real system y (sensor measurements), against the outputs given by a related mathematical model $\hat{y}$, while a performance criterion that quantifies the value of the approximation error is used. Therefore, the optimization task relies on finding a set of values of the burst parameters minimizing a criterion function of the estimation error.

In order to evaluate (9), it is necessary to count with the values of $z_L(k)$, $H_2(k)$ and $\lambda(k)$ since these are unknown and correspond directly to the solution of the BDL problem. In this way, the proposed extended DE algorithm is used to estimate such values, using a population of candidate solutions of the form $\chi(i, g) = [\widehat{z_L}(k, i, g) \;\; \widehat{H_2}(k, i, g) \;\; \hat{\lambda}(k, i, g)]^T$. Now, considering the measurements $Q_1(k)$ and $Q_3(k)$, and its estimations $\widehat{Q_1}(k)$ and $\widehat{Q_3}(k)$ given by (9), it is possible to establish a performance measure in order to quantify how close $\hat{y}$ is from y, for each candidate solution. So, model (9) is completed by using the values obtained by the proposed algorithm and then, the performance of each $\chi(i, g)$ is evaluated by the cost function (14) in order to select the best candidate solution:

$$f_c(y(k), \hat{y}(k)) = \frac{1}{2}\|y(k) - \hat{y}\ (k)\|^2 \tag{14}$$

where $y(k) = [Q_1(k) \;\; Q_3(k)]^T$ and $\hat{y}(k) = [\widehat{Q_1}(k) \;\; \widehat{Q_3}\ (k)]^T$, in order to select the best candidate solution.

The BDL problem can be expressed as an optimization task as:

$$\begin{aligned} &\min_{\chi \in S} f_c(y(k), \hat{y}(k)) \\ &\text{subject to:} \quad x(k+1) = \xi_d(x(k), u(k), u(k+1)), \\ &\qquad\qquad\quad y(k) = Cx(k), \\ &\qquad\qquad\quad \chi_1^{\text{low}} \le \chi_1 \le \chi_1^{\text{up}}, \\ &\qquad\qquad\quad \chi_2^{\text{low}} \le \chi_2 \le \chi_2^{\text{up}}, \\ &\qquad\qquad\quad \chi_3^{\text{low}} \le \chi_3 \le \chi_3^{\text{up}} \end{aligned} \tag{15}$$

where S is the feasible space and χ^{up} and χ^{low} are the lower and upper bounds for each parameter to be estimated.

The following subsections present three strategies that allow to extend the classical DE algorithm in order to tackle the BDL problem efficiently.

Initial bounds of the search space

Before the population of the DE algorithm can be initialized, both upper χ^{up} and lower χ^{low} bounds for all the candidate solutions must be specified. In this case, for each characteristic of the burst, there is a certain range within which the value of the bounds should be restricted, due to its physical correspondence. A good definition of the feasible search space and their boundaries provides extra knowledge about the optimization problem, making the deployment of the algorithm faster and efficient (avoiding the consideration of unfeasible candidate solutions). The BDL problem is defined by the unknown values of the burst position, pressure and magnitude of model (9), whose physical boundaries are included in Table 1.

In Table 1, ϵ_m is selected as 0.001 in order to guarantee the numerical stability of the algorithm. On the other hand, it is clear that the upper bound for the burst position is a

Table 1 | Unknown burst parameters

Parameter	Symbol	Upper bound	Lower bound	Units
Burst position	z_L	$L_{\text{eq}} - \epsilon_m$	ϵ_m	$[m]$
Burst pressure	H_2	H_3	H_1	$[m]$
Magnitude factor	λ	λ_U	ϵ_m	$[m^{5/2}/s]$

value near to the total length of the pipeline and the pressure at the burst point must be between the inlet and outlet pressure. However, in order to define the upper bound of the magnitude factor (λ), it is necessary to determine the maximum tolerable crack size before a total fracture of the pipeline occurs. Under this consideration, the upper bound of the magnitude factor is given by:

$$\lambda_U = \frac{C_d(\pi e_c^2)}{4\sqrt{2g}} \tag{16}$$

where e_c is the stable grow crack size supported by the pipe and C_d is a discharge coefficient that can be selected near to 1.

When a burst localization method is used, it is desirable that the orifice or rupture remains stable in order to provide sufficient time to isolate and repair it. The analysis that describes the necessary conditions for this situation is known as *Leak-Before-Break* (LBB) criterion. A basic analysis, based on Linear Elastic Fracture Mechanics (LEFM), to establish the LBB criterion is presented by Anderson (2017). Considering this, the crack size will remain stable if:

$$e_c = \frac{K_{Ic}^2}{(\pi\sigma_p)^2} \tag{17}$$

where K_{IC} is the fracture toughness of the pipe material $[\text{Pa}(m)^{1/2}]$, and σ_p is the operating hoop stress [Pa], calculated as $\sigma_p = PD/2e$, where P is the operating pressure [Pa].

Calibration zone

One of the main difficulties that a user faces when a heuristic algorithm is applied is to select an appropriate set of synthesis parameters (Lobo *et al.* 2007). In the case of the DE algorithm, the main synthesis parameters that are required are the *Mutation Factor* F and the *Recombination Crossover* C_r, whose selection is crucial for a correct algorithm performance.

In order to obtain adequate synthesis parameters of the DE algorithm, addressing the BDL problem, this work follows the methodology called by its authors (Peréz-González *et al.* 2016) *Comfort Zone* (CZ). This methodology consists in evaluating the performance of the DE algorithm, in a particular case, under an iterative execution that uses different parameter settings (F, C_r), selected by means of the expression:

$$\begin{aligned} F &= 0.0001 + (2 - 0.0001)\text{rand}(1) \\ C_r &= 0.0001 + (1 - 0.0001)\text{rand}(1) \end{aligned} \tag{18}$$

where the lower bounds in both cases are 0.0001 in order to guarantee numerical stability and the upper bounds of F and C_r are 2 and 1, respectively, in agreement with Price *et al.* (2006). The information obtained from the CZ allows a relationship to be established between the calibration and performance of an algorithm, providing a statistical measurement of the probability to obtain a high-performance execution by using a calibration setting that lies in a specific region. Of course, the intention is to use the calibration settings that present the higher probabilities of providing good performance for the algorithm. In this case, the number of iterations needed to reach a specific error bound is defined as a performance measure of the algorithm.

Multi-start scheme

In Equation (9), the pressure at the burst point $H_2(k)$ corresponds to a *state* of the model, which turns the optimization task into a dynamic optimization problem. That is, the proposed algorithm must track the dynamic behavior of $H_2(k)$ at each instant of the sampling time. In order to do that, the use of a multi-start scheme is proposed (Branke 2012), that allows consideration of the evaluation of model (9), in each sampling time k, as an independent optimization problem. So, for the k-th sample, there exists a set of values $\{z_L(k),\ H_2(k),\ \lambda(k)\}$ that minimizes (14), therefore, the DE algorithm estimates these values. Before the dataset that corresponds to the sampling time $k+1$ arrives, the DE

algorithm is initialized and iterated in order to solve the optimization problem represented by the dataset sampled in the k-th interval of time. With this solution, the arrival of the $k+1$ sample set is allowed and the DE algorithm starts again over it, taking this new configuration as a new optimization problem. Of course, tackling a single optimization problem in each sampling time is computationally expensive, nevertheless, the set CZ offers a statistical guarantee of reaching a good solution in a low number of iterations, which makes it easier to execute the optimization scheme as a set of independent optimization tasks.

Finally, the proposed DE algorithm to address the BDL problem can be illustrated by the pseudocode presented in the Appendix section (available with the online version of this paper).

EXPERIMENTS AND RESULTS

Prototype description

The BDL methodology based on the extended DE algorithm is evaluated using datasets acquired from the prototype built at the Center for Research and Advanced Studies (Cinvestav), located in Guadalajara, México. Figure 2 presents the prototype diagram and Table 2 contains the physical parameters of the prototype. This pipeline consists of a Polypropylene Random Copolymer circuit of pipes, supplied by a water tank (T1) through a centrifugal pump (FB1), which is controlled by a variable frequency driver of

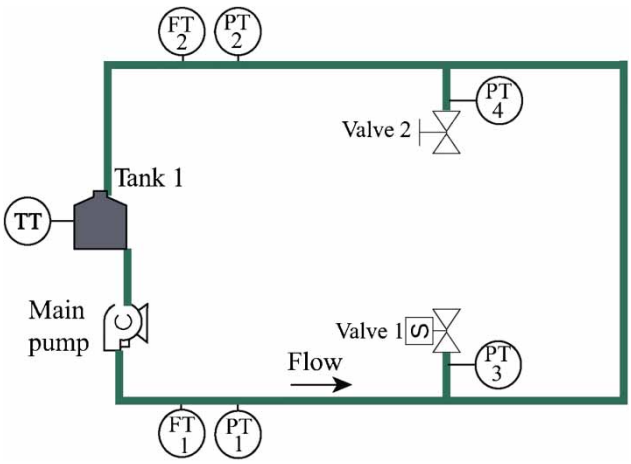

Figure 2 | Pipeline prototype diagram.

Table 2 | Pipeline physical parameters

Parameter	Symbol	Value	Units
Length between sensors	L_r	68.147	$[m]$
Roughness	ε	7.0×10^{-6}	$[m]$
Internal diameter	D	6.271×10^{-2}	$[m]$
Wall thickness	e	13.095×10^{-3}	$[m]$
Young modulus	E	7.008×10^{8}	$[Pa]$
Slope	θ	0	$[deg]$

0−60 Hz. The flow rate and pressure head at the ends of the pipeline are measured by means of two ultrasonic flow sensors *Promag Propiline 10P* (FT1 and FT2) and two pressure sensors *PMP 41* (PT1 and PT2), respectively. The temperature is measured by means of a resistive sensor *PT100* (TT1). The prototype also has one electrovalve and a manual ball-type valve, whose diameter is 0.0127 m, which allow to emulate a burst in their locations: 17.045 m (valve 1) and 49.895 m (valve 2). Each valve also has a pressure sensor (PT3 and PT4) that allows validation of the pressure estimations in the points of each emulated burst. Pictures of some components of the described prototype can be found in https://www.gdl.cinvestav.mx/ofelia/index.php?page=fdg (accessed March 17, 2019).

In this research, the data acquisition is performed by a *NI-myRIO*-embedded device. This system is equipped with a *Xilinx Zynq-7010 FPGA* and a dual-core ARM CortexTM processor. The computational processing of the acquired data is carried out by means of a desktop computer equipped with an IntelCore™ i7-2600 K, 3.4 GHz processor, 15.7 GB of *RAM*, and Windows™ 10 PRO edition OS, including LabView™ 2016 myRIO-oriented software.

In the diagram, the sensors FT1 and FT2 acquire the flow measurements Q_{in} and Q_{out}, respectively, and the sensors PT1 and PT2 acquire the pressure measurements H_{in} and H_{out}, respectively.

Setup and settings

Before the execution and evaluation of the extended DE algorithm in the BDL problem, the synthesis parameters are defined. First, the value of λ_U by using (15) is 0.4 m, considering a fracture toughness (K_{IC}) of 0.7 MPa$(m)^{1/2}$, an operating pressure (P) of 176.514 kPa and a discharge

coefficient (C_d) of 0.9. Second, the pressure wave speed is determined. Despite the fact that valid results of burst localization have been obtained in publications such as Delgado-Aguiñaga *et al.* (2015), Delgado-Aguiñaga & Begovich (2017), and Lizarraga-Raygoza *et al.* (2018), in this work attempting to find improved results, the pressure wave speed is experimentally determined as in Pérez-González *et al.* (2019). In the experiment, a burst is produced by a valve with known position and then the difference between instants of time where the pressure waves arrive at the pressure sensors located at the ends of the pipeline are registered. Once the time instants are obtained, the wave speed is estimated as:

$$a = \frac{-(L_r - 2z_r) \pm \sqrt{(L_r - 2z_r) + (V^2\Delta t - VL_r)}}{2\Delta t} \tag{19}$$

where L_r is the distance between pressure sensors, z_r is the known valve position, V is the fluid velocity and Δt is the difference of times t_1 and t_2 in which the pressure drop, generated by the burst, arrives at the upstream and downstream sensors, respectively. In order to estimate the arrival time of the pressure wave to the sensors, a Discrete Wavelet Transform (DWT) method is used as in Romero-Delgado & Begovich (2017). With the only purpose to calibrate the pressure wave speed, a burst is produced by means of the valve 1 (located at 17.045 m) under the experimental conditions of the Table 3. As result of this experiment, a pressure wave speed value 355.914 m/s is obtained.

On the other hand, in order to find the suitable synthesis parameters F and C_r of the algorithm to address the BDL problem, the CZ procedure is performed. In this way, the algorithm is executed in an iterative way on the acquired data from the pipeline prototype by producing a burst by the valve 1. To define the CZ, a cost function based on the total mean square error is considered for each execution:

$$f_{\text{MSE}} = \frac{1}{2K}\sum_{k=1}^{K}(Q_1(k) - \widehat{Q_1}(k))^2 \quad + (Q_3(k) - \widehat{Q_3}(k))^2 \tag{20}$$

where K is the total number of samples in a database. It is expected that the proposed algorithm reaches a good estimation of the burst parameters at the end of each execution, allowing a maximum number of 500 iterations in each execution. In addition to this, an execution is considered *successful* when the algorithm reaches an error bound defined as $f_{\text{MSE}} \leq 1 \times 10^{-12}$ in less than 20 iterations, as *poor execution* when the algorithm reaches the error bound in more than 20 iterations, but less than 500 and as *failed execution* when the algorithm does not reach the error bound, even with 500 iterations. The results obtained after 1000 executions are shown in Figure 3. The circles correspond to the successful executions and the squares the failed executions. The successful executions represent 18% of the total of the executions. As Figure 3 shows, when the parameters F and C_r are specified arbitrarily, there is a great probability to obtain a bad performance. On the other hand, it can also be seen that there is an interval of F and C_r where the ED algorithm presents a good performance.

The successful executions are distributed between the regions: $0.40 \leq F \leq 1.20$ and $0.6 \leq C_r \leq 0.95$. The minimum value of iterations needed to reach the error bound is 14, obtained by using $F = 0.53$ and $C_r = 0.85$.

Once the CZ is determined, the parameters setting for the implementation of the DE algorithm is taken as $NP = 30$, since for many applications, the population size is taken as $NP = 10d$, as it is reported in Price (1997). The control parameters $C_r = 0.53$, $F = 0.85$ obtained from the CZ are used, and a total of 20 iterations per sample are considered. Finally, in order to detect the presence of a burst, and in consequence, start the algorithm, the burst detection alarm is established when the expression $|Q_1(k) - Q_2(k)| \geq 0.5 \times 10^{-4}$ becomes true, in order to avoid the uncertainty in the flow measurement introduced by the noise level of the sensors.

It is important to point out that the model-based burst diagnosis methods present high dependence to some pipeline

Table 3 | Experimental test conditions to pressure wave speed estimation

Steady flow [m^3/s]	Temperature [°C]	L_r [m]	V [m/s]	z_r [m]	t_1 [s]	t_2 [s]
8.892	24.31	68.147	2.8906	17.045	30.540	30.631

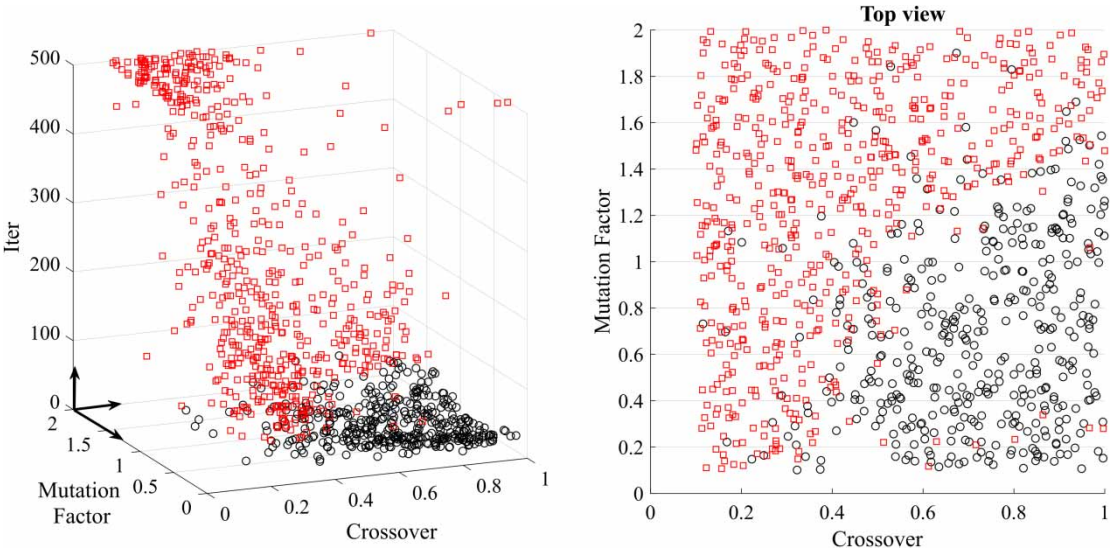

Figure 3 | CZ for the BDL problem.

parameters, such as the friction and diameter, then it is necessary to periodically calibrate the pipeline parameter.

RESULTS AND DISCUSSION

In order to show the performance of the proposed algorithm in the BDL problem, this subsection presents two different experiments using real data from the prototype described above. In addition to this, the proposed algorithm is compared against the EKF, as one of the most widely used algorithms that presents good performance in the BDL problem (Delgado-Aguiñaga *et al.* 2016).

In *Experiment 1*, a single burst is emulated under constant flow conditions, by means of the valve 2, located at 49.895 m at time $t_L = 104$ s. The mean temperature during the experiment is 24.31°C and the mean viscosity is 9.0641 [*unitless*]. The pressure head and flow rate at the ends of the pipeline are shown in Figure 4 and the experimental conditions are presented in Table 4.

After the burst occurrences, two friction factors and Reynolds numbers are estimated with the input and output flows. In this experiment, $f(Q1) = 0.015513$ and $f(Q2) = 0.015786$. On the other hand, we have $R_e(Q_1) = 2.0263 \times 10^5$ and $R_e(Q_2) = 1.8529 \times 10^5$.

The results obtained from Experiment 1 with the extended DE algorithm and with the EKF are shown in

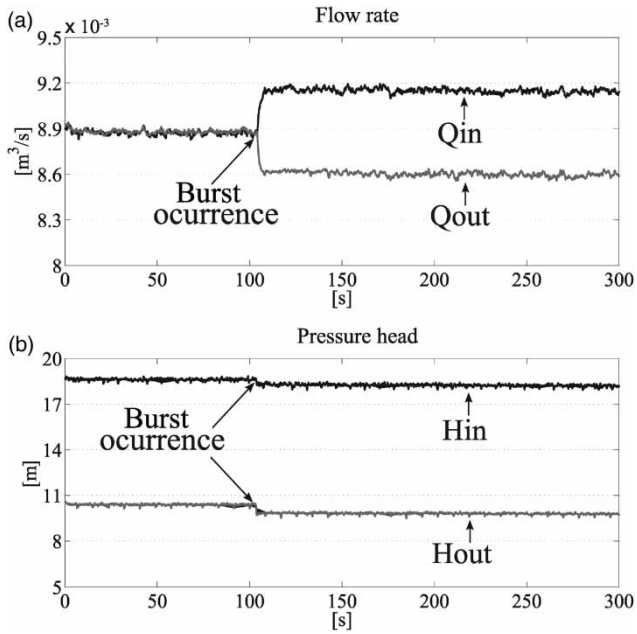

Figure 4 | Flow rate and pressure head at the ends of the pipeline (Experiment 1).

Figure 5: (a) presents the real burst position z_L and its estimation with the proposed DE algorithm and the EKF; the real pressure head H_2 and its estimation are shown in (b), and finally, the magnitude factor λ and its estimation are presented in (c). As it is shown in Figure 5, the burst value estimations obtained from the extended DE algorithm and the EKF are close to the real values.

Table 4 | Mean values of the first experiment

Experiment parameter/signal	Symbol	Value before the burst occurrence	Value after the burst occurrence	Units
Input pressure head	H_1	18.8390	18.1460	$[m]$
Output pressure head	H_3	10.4795	9.982936	$[m]$
Input flow rate	Q_1	0.00892	0.00949	$[m^3/s]$
Output flow rate	Q_2	0.00891	0.00868	$[m^3/s]$
Reynolds number	R_e	1.9042×10^5	See text below	$[unitless]$
Friction factor	f	0.015516	See text below	$[unitless]$

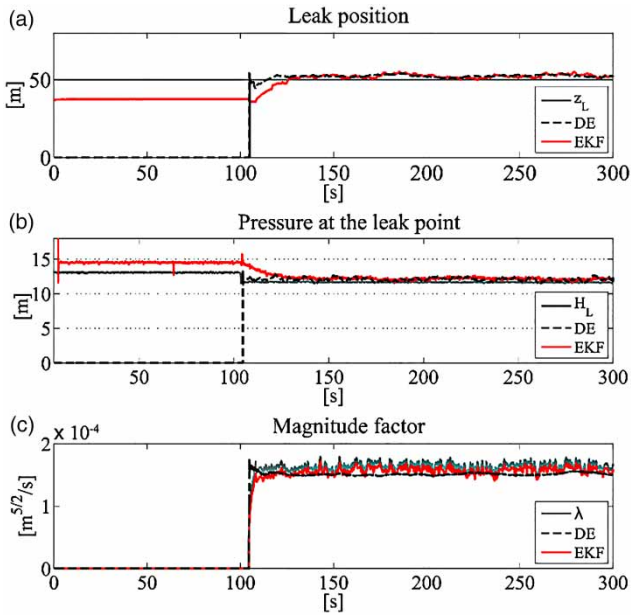

Figure 5 | Burst values and their estimations in Experiment 1.

In order to validate the obtained estimations, Figure 6 shows the comparison between the measured flows and their estimations given by model (9), obtained by the incorporation of the best parameters found by the extended DE algorithm at each sample.

Table 5 presents the average, root mean square error (RMSE) and standard deviation (STD) of each estimated value obtained with the extended DE and EKF algorithms, considering a time interval between 130 s and 300 s.

A *second experiment* is performed, in order to highlight the effectiveness of the proposed method. A new burst is

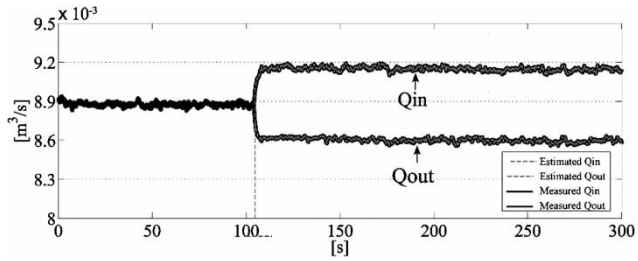

Figure 6 | Flow measures and their estimations in Experiment 1.

Table 5 | Estimated parameters in Experiment 1

Method	Parameter	Real value	Average estimation	Max. STD	RMSE
Differential Evolution	$z_L[m]$	49.895	47.856	1.94	2.474
	$H_2[m]$	11.147	12.107	0.162	0.975
	$\lambda[m^{5/2}/s]$	1.65×10^{-4}	1.49×10^{-4}	1.17×10^{-6}	1.63×10^{-5}
Extended Kalman Filter	$z_L[m]$	49.895	47.306	0.813	2.277
	$H_2[m]$	11.147	12.222	0.0932	1.060
	$\lambda[m^{5/2}/s]$	1.65×10^{-4}	1.56×10^{-4}	7.85×10^{-6}	7.37×10^{-6}

emulated using again the valve 2 (49.895 m) at time $t_L = 40$ s, but also, producing variations in the operation point of the pump, by means of the frequency driver. Figure 7

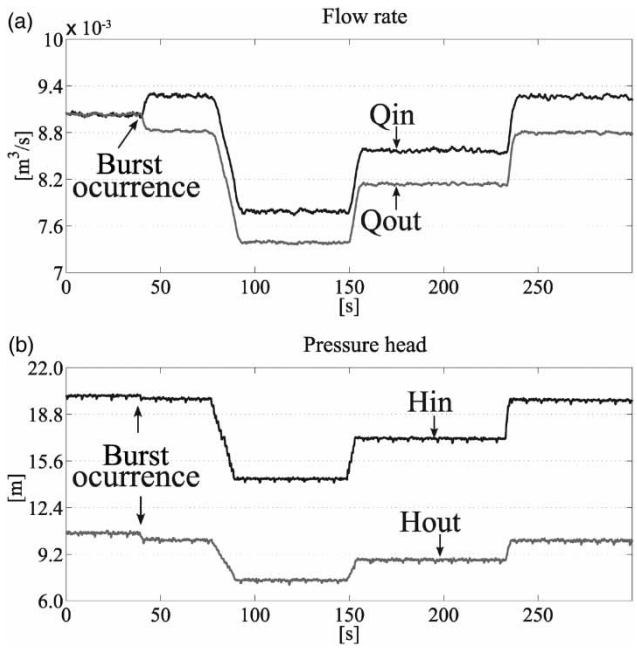

Figure 7 | Flow rate and pressure head at the ends of the pipeline (Experiment 2).

shows the dataset used during this new experiment and Table 6 presents the experimental scenario.

In this experiment, the variation range of the friction factors $f(Q1)$ and $f(Q2)$ are $[0.0150 - 0.0156]$ and $[0.0149 - 0.0154]$, respectively. On the other hand, the variation ranges of the Reynolds numbers $R_e(Q_1)$ and $R_e(Q_2)$ are $[2.06142 \times 10^5 - 2.4796 \times 10^5]$ and $[2.3701 \times 10^5 - 1.9610 \times 10^5]$, respectively.

Figure 8 shows the estimation results during the second experiment. The plot (a) presents the estimation of z_L, where the estimated position of the burst point does not change in spite of the variations in the operating point of the pump. In this way, the estimation of z_L maintains its behavior in the neighborhood of the real value with a displacement of 1.45%. The same behavior is presented by the magnitude factor, presenting a displacement of 8.23% with respect to the real value of 1.326×10^{-4} as Figure 8(c) shows. The case of the pressure head at the leak point is different from the previous two, since H_2 changes with respect to the variations of the operation point, despite this, the proposed extended DE algorithm can follow the dynamic variations.

In order to validate the obtained estimations, Figure 9 shows the comparison between the measured flows and their estimations given by Equation (9) considering the best parameters found by the extended DE algorithm at each sample.

Table 6 | Mean values of the second experiment

Experiment parameter/signal	Symbol	Value before the burst occurrence	Value after the burst occurrence (variation range)	Units
Input pressure head	H_1	20.0513	14.116–19.9137	$[m]$
Output pressure head	H_3	10.6329	7.0705–10.3411	$[m]$
Input flow rate	Q_1	0.0090	0.0077–0.0093	$[m^3/s]$
Output flow rate	Q_2	0.0090	0.0073–0.0088	$[m^3/s]$
Reynolds number	R_e	2.4059×10^5	See text below	$[unitless]$
Friction factor	f	0.014944	See text below	$[unitless]$

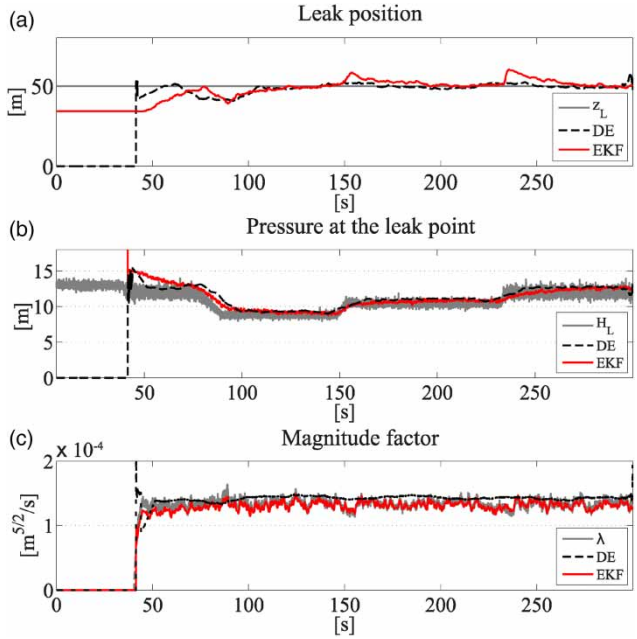

Figure 8 | Burst values and their estimations in Experiment 2.

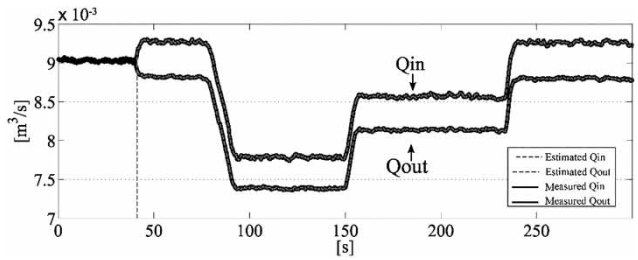

Figure 9 | Flow measures and their estimations in Experiment 2.

Table 7 summarizes the obtained results and their corresponding statistical values, considering a time interval between 130 s and 300 s.

Remember that in Experiment 2, the head pressure H_2 after the burst occurrence is not constant and considering this condition the average value is not expressed. However, in Figure 8(c), it is possible to see that the pressure variations are well estimated.

The results obtained from the performed experiments show that the proposed extended DE algorithm offers similar results than the EKF. Nevertheless, in the first experiment, the burst position presents a lower STD with the EKF, in contrast, in the second experiment, the STD is less with the DE algorithm. This fact shows that the data

Table 7 | Estimated parameters in Experiment 2

Method	Parameter	Real value	Average estimation	max STD	RMSE
Differential Evolution	$z_L[m]$	49.895	49.386	0.610	2.25
	$H_2[m]$	See text below	See text below	0.430	0.722
	$\lambda[m^{5/2}/s]$	1.32×10^{-4}	1.431×10^{-4}	1.19×10^{-4}	1.255×10^{-5}
Extended Kalman Filter	$z_L[m]$	49.895	51.863	1.016	3.224
	$H_2[m]$	See text below	See text below	0.387	0.523
	$\lambda[m^{5/2}/s]$	1.327×10^{-4}	1.316×10^{-4}	5.793×10^{-6}	3.201×10^{-6}

fusion of multiple algorithms could reduce the uncertainty degree provided by an individual estimation.

The extended DE algorithm presents additional advantages since it requires only a few samples to approximate a solution and it does not need a linearization of the mathematical model, as the EKF does, simplifying in this way the implementation. However, like most evolutive algorithms, its real-time implementation is limited by the computational cost of each iteration in relation to the available time between samples, in this case, the mean computational time per iteration of the ED algorithm is 0.00366 s, while the EKF only takes 5.6625×10^{-5} s. Furthermore, it is necessary to emphasize that the correct definition of the search space and the adequate selection of the synthesis parameters of the DE algorithm allow to reach a good estimation of the burst values and also the multi-start scheme provides a powerful tool in order to deal with dynamic optimization.

CONCLUSIONS

In this paper, an extended version of the DE algorithm is proposed to address the burst detection and localization problem, where the problem relies on estimating the parameters related to a burst occurrence. The experimental results obtained from the used pipeline prototype show that the proposed DE algorithm is a suitable method to estimate the burst parameters under different practical scenarios. In addition to this, it is important to point out that the correct definition of the search space, as well as the synthesis parameters of the DE algorithm, play a fundamental role to achieve an adequate estimation of the burst parameters. Moreover, the estimation of the burst parameters provided by the DE algorithm is similar to the ones provided by the EKF. This fact allows to consider the DE algorithm as a useful element for the conformation of a bank of burst diagnosers, as a strategy that provides more informed and reliable burst detection and localization. As future work, the heuristic techniques can be included in more complex BDL problems, such as multiple burst diagnosis and branched pipes.

REFERENCES

Anderson, T. L. 2017 *Fracture Mechanics, Fundamentals and Applications*. CRC Press, Boca Raton, CA.

Badillo-Olvera, A., Begovich, O. & Peréz-González, A. 2017 Leak isolation in pressurized pipelines using an interpolation function to approximate the fitting losses. *J. Phys. Conf. Ser.* **783** (1), 012012.

Branke, J. 2012 *Evolutionary Optimization in Dynamic Environments*. Springer Science & Business Media, Heidelberg.

Brunone, B., Golia, U. M. & Greco, M. 1995 Effects of two-dimensionality on pipe transients modeling. *J. Hydraul. Eng.* **121**, 906–912.

Brunone, B., Meniconi, S., Capponi, C. & Ferrante, M. 2015 Leak-induced pressure decay during transients in viscoelastic pipes. Preliminary results. *Procedia Engineering* **119**, 243–252.

Brunone, B., Meniconi, S. & Capponi, C. 2018 Numerical analysis of the transient pressure damping in a single polymeric pipe with a leak. *Urban Water J.* **15** (8), 760–868.

Carvajal-Rubio, J. E. & Begovich, O. 2016 Bank of leak diagnosis algorithms for pressurized pipelines. In: *13th International Conference on Electrical Engineering, Computing Science and Automatic Control (CCE)*. IEEE, pp. 1–6.

Chaudhry, M. H. 2014 *Applied Hydraulic Transients*. Springer, New York.

Coello, C., Lamont, G. & Van Veldhuizen, D. A. 2007 *Evolutionary Algorithms for Solving Multi-Objective Problems*. Springer Science & Business Media, New York.

Delgado-Aguiñaga, J. A. & Begovich, O. 2017 Water leak diagnosis in pressurized pipelines: a real case study. In: *Modeling and Monitoring of Pipelines and Networks*. Springer, Cham, pp. 235–262.

Delgado-Aguiñaga, J., Besançon, G. & Begovich, O. 2015 Leak isolation based on Extended Kalman Filter in a plastic pipeline under temperature variations with real-data validation. In: *23rd Mediterranean Conference on Control and Automation (MED)*. IEEE, pp. 316–321.

Delgado-Aguiñaga, J. A., Besançon, G., Begovich, O. & Carvajal, J. E. 2016 Multi-leak diagnosis in pipelines based on Extended Kalman Filter. *Control Eng. Pract.* **49**, 139–148. https://doi.org/10.1016/j.conengprac.2015.10.008.

Duan, H. F., Meniconi, S., Lee, P. J., Brunone, B. & Ghidaoui, M. S. 2017 Local and integral energy-based evaluation for the unsteady friction relevance in transient pipe flows. *J. Hydraul. Eng.* **143**, 04017015.

Dulhoste, J.-F., Besançon, G., Torres, L., Begovich, O. & Navarro, A. 2011 About friction modeling for observer-based leak estimation in pipelines. In: *50th IEEE Conference on Decision and Control and European Control Conference*. IEEE, pp. 4413–4418.

Dulhoste, J. F., Guillén, M., Besançon, G. & Santos, R. 2017 One-dimensional modeling of pipeline transients. In: *Modeling and Monitoring of Pipelines and Networks*. Springer, Cham, pp. 63–81.

Evangelista, S., Leopardi, A., Pignatelli, R. & de Marinis, G. 2015 Hydraulic transients in viscoelastic branched pipelines. *J. Hydraul. Eng.* **141**, 04015016.

Ferrante, M., Brunone, B., Meniconi, S., Capponi, C. & Massari, C. 2014 The leak law: from local to global scale. *Procedia Eng.* **70**, 651–659.

Kowalczuk, Z. & Gunawickrama, K. 2004 Detecting and locating leaks in transmission pipelines. In: *Fault Diagnosis*. Springer, Berlin, pp. 821–864.

Lizarraga-Raygoza, A., Delgado-Aguiñaga, J. A. & Begovich, O. 2018 Steady state algorithm for leak diagnosis in water pipeline systems. *IFAC-Pap.* **51**, 402–407.

Lobo, F. J., Lima, C. F. & Michalewicz, Z. 2007 *Parameter Setting in Evolutionary Algorithms*. Springer Science & Business Media, Berlin.

Mataix, C. 1982 *Mecánica de Fluidos Y Máquinas Hidráulicas*. Oxford University Press, Mexico.

Meniconi, S., Brunone, B., Ferrante, M., Capponi, C., Carrettini, C. A., Chiesa, C., Segalini, D. & Lanfranchi, E. A. 2015 Anomaly pre-localization in distribution–transmission mains by pump trip, preliminary field tests in the Milan pipe system. *J. Hydroinformatics* **17**, 377–389.

Navarro, A., Begovich, O., Sánchez, J. & Besancon, G. 2017 Real-time leak isolation based on state estimation with fitting loss coefficient calibration in a plastic pipeline. *Asian J. Control* **19**, 255–265.

Peréz-González, A., Begovich, O. & Ruíz-León, J. 2016 Evolutive extension: a biological approach to heuristic algorithms. In: *Paper presented at the Proceedings of the Latin American Conference on Automatic Control, XVII CLCA*. pp. 373–378.

Pérez-González, A., Badillo-Olvera, A., Begovich-Mendoza, O. & Ruíz-León, J. 2019 Calibration zone for the parameters of the differential evolution algorithm and its application to a real burst location problem. *J. Fluids Eng.* **141** (5), in press.

Price, K. V. 1997 Differential evolution vs. the functions of the 2/sup nd/ICEO. In: *IEEE International Conference on Evolutionary Computation*. IEEE, pp. 153–157.

Price, K., Storn, R. M. & Lampinen, J. A. 2006 *Differential Evolution: A Practical Approach to Global Optimization*. Springer Science & Business Media, Berlin.

Roberson, J. A., Cassidy, J. J. & Chaudhry, M. H. 1998 *Hydraulic Engineering*. Wiley, New York.

Romero-Delgado, M. & Begovich, O. 2017 A comparison between leak location methods based on the negative pressure wave. In: *14th International Conference on Electrical Engineering, Computing Science and Automatic Control (CCE)*. IEEE, pp. 1–6.

Santos-Ruiz, I., Bermúdez, J. R., López-Estrada, F. R., Puig, V., Torres, L. & Delgado-Aguiñaga, J. A. 2018 Online leak diagnosis in pipelines using an EKF-based and steady-state mixed approach. *Control Eng. Pract.* **81**, 55–64.

Soares, A. K., Covas, D. I. & Reis, L. F. 2008 Analysis of PVC pipe-wall viscoelasticity during water hammer. *J. Hydraul. Eng.* **134**, 1389–1394.

Suribabu, C. R. 2010 Differential evolution algorithm for optimal design of water distribution networks. *J. Hydroinformatics* **12**, 66.

Torres, L., Verde, C., Besancon, G. & Gonzalez, O. 2014 High-gain observers for leak location in subterranean pipelines of liquefied petroleum gas. *Int. J. Robust Nonlinear Control* **24**, 1127–1141.

Verde, C. 2001 Multi-leak detection and isolation in fluid pipelines. *Control Eng. Pract.* **9**, 673–682.

Verde, C. & Torres, L. 2017 *Modeling and Monitoring of Pipelines and Networks*. Springer, Cham.

Wang, X.-J., Lambert, M. F., Simpson, A. R., Liggett, J. A. & Vítkovský, J. P. 2002 Leak detection in pipelines using the damping of fluid transients. *J. Hydraul. Eng.* **128**, 697–711.

Xie, X., Zhou, Q., Hou, D. & Zhang, H. 2017 Compressed sensing based optimal sensor placement for leak localization in water distribution networks. *J. Hydroinformatics* **20** (6), 1286–1295.

Zhang, J. & Sanderson, A. C. 2009 JADE: adaptive differential evolution with optional external archive. *IEEE Trans. Evol. Comput.* **13**, 945–958.

Zheng, F., Simpson, A. R. & Zecchin, A. 2011 Performance study of differential evolution with various mutation strategies applied to water distribution system optimization. In: *World Environmental and Water Resources Congress 2011, Bearing Knowledge for Sustainability*. ASCE, Palm Springs, pp. 166–176.

First received 1 November 2018; accepted in revised form 16 March 2019. Available online 1 April 2019